Planar Josephson Junctions Fabricated With Magnesium Diboride Films

D. A. Kahler, J. Talvacchio, J. M. Murduck, A. Kirschenbaum, R. E. Brooks, S. B. Bu, J. Choi, D. M. Kim, and C.-B. Eom

***Abstract*—Josephson junctions were fabricated in three planar configurations using a focused ion beam (FIB) to cut $\geq$70 nm gaps in MgB_2 bridges. In two of the approaches—narrowed microbridges where a 0.1 μm bridge was left in place after the FIB cut or thinned microbridges where a 20–40 nm-thick film layer remained uncut—we reproduced junction results obtained by other researchers but with $I_c(T) > 0$ at substantially higher temperatures, $>$32 K. Measurements were made of critical current modulation in an applied magnetic field and I–V curves were measured with the chips exposed to 1–10 GHz radiation. In the third configuration, S-N-S structures were made by filling the gap made by the FIB with a noble metal. This configuration is preferred to S-S'-S since the normal-conductor coherence length of 40–100 nm for a clean metal roughly matches the width of the FIB cut. Junction R_n measurements showed that ex-situ Au deposited after a low-energy argon ion cleaning was not as effective as in-situ Pt deposition for obtaining low-resistance S-N interfaces.**

***Index Terms*—Josephson junction, magnesium diboride, superconductor.**

I. Introduction

SINCE the discovery of magnesium diboride (MgB_2) as a superconductor in 2001 [1], there has been interest in fabricating junctions of this material. MgB_2 is attractive because it has a relatively high transition temperature of 39 K, four times that of Nb and 2–3 times that of NbN. In contrast to the high-T_c oxides where nodes in the superconducting energy gap appear to suppress the I_cR_n products of junctions, MgB_2 junctions have a potential for I_cR_n products and THz switching speeds that roughly scale with T_c compared to Nb or NbN while operating at about 25 K.

Many of the configurations that have been used in making junctions in the high-T_c oxides are also candidates for MgB_2 junctions, except that MgB_2 grain boundaries do not exhibit weak coupling effects and MgB_2 may not be as sensitive to electron or ion damage. In addition, MgB_2 films are just starting to be deposited in multilayer film structures so we were restricted to planar configurations with just one MgB_2 film layer.

This paper discusses the fabrication and results on three planar junction configurations that are shown schematically in Fig. 1(a), (b), and (c)–(f), respectively, and that can be described as a thinned microbridge, narrowed microbridge, and a Superconductor-Normal-Superconductor or SNS structure. Results on thinned [2] and narrowed [3] microbridges made in somewhat lower-T_c MgB_2 films have been reported by other laboratories. We argue that the SNS structures have greater potential for high I_cR_n products so we explored several versions. Our investigation is limited to junctions for large-scale circuit integration so we did not consider junctions fabricated in bulk materials as in [4].

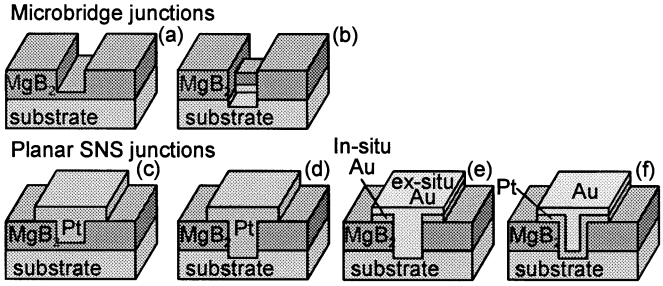

Fig. 1. Planar configurations for MgB_2 junctions.

II. Experiment

The process for depositing MgB_2 thin films is described in detail in [5]. Briefly, boron films were sputtered onto Al_2O_3(0001) substrates and then annealed at 850°C in magnesium vapor. Films were 200–250 nm thick to exceed the magnetic penetration depth of MgB_2 [6] as will ultimately be required for circuits.

Before patterning, all films had a gold contact layer deposited. In the case of devices with the configuration shown in Fig. 1(e), we used x-ray photoelectron spectroscopy (XPS) to determine that the reaction products with air were completely removed by argon ion milling before depositing the Au contact layer in-situ.

Two photomasks and 150 eV argon ion milling were used to define 2 to 20-μm-wide bridges in the MgB_2/Au bilayer and then to remove unneeded Au, respectively. A quarter of a patterned chip is shown in Fig. 2(a). Two concentric subchips are shown with 44 contact pads for each—2 pads to contact a common electrode and 21 pairs of contacts to permit four-point measurements to be made on 21devices. Fig. 3 shows uniformity in critical current (I_c) vs. temperature for a complete set of 10-μm-wide by 250-nm-thick MgB_2 bridges before any junctions were patterned.

Manuscript received August 5, 2002. This work was supported in part by AFOSR under Contract F49620-02-1-0046.

D. A. Kahler, J. Talvacchio, J. M. Murduck, A. Kirschenbaum, and R. E. Brooks are with Northrop Grumman Advanced Technology Center, Baltimore, MD 21090 USA (e-mail: kahleda@md.northgrum.com).

S. B. Bu, J. Choi, D. M. Kim, and C.-B. Eom are with the University of Wisconsin, Madison, WI 53706 USA (e-mail: eom@engr.wisc.edu).

Digital Object Identifier 10.1109/TASC.2003.814152

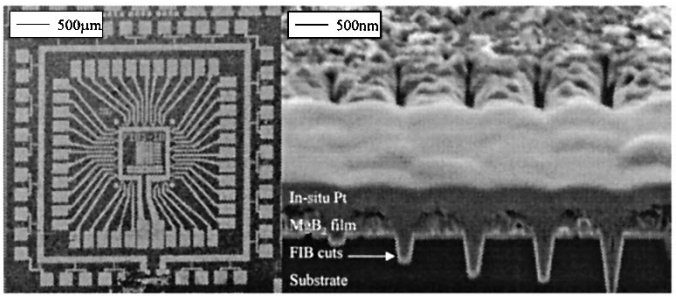

(a) (b)

Fig. 2. (a) Patterned MgB_2 subchip showing two concentric rings of 21devices each. (b) Cross-sectional view of five test FIB cuts with in-situ deposited Pt filling the volume where MgB_2 was removed.

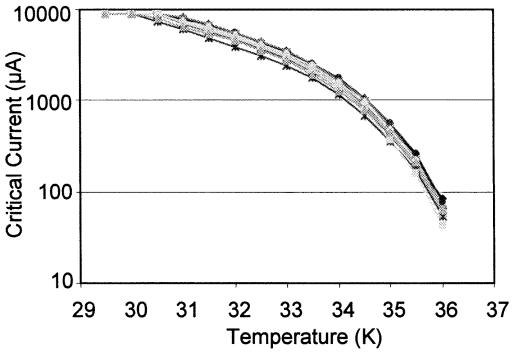

Fig. 3. Critical current vs. temperature for a subchip with 10 μm $\times$ 250 nm-thick patterned bridges showing the uniformity of the MgB_2 film and no film degradation from photolithographic processing. The highest available measurement current was 9 mA.

Junctions were patterned by cutting into the MgB_2 bridges using a 30 keV, 72 pA focused Ga ion beam (FIB). FIB processing parameters for one subchip are shown in Table I. In this case, we patterned thinned microbridges, narrowed microbridges and SNS junctions with in-situ-deposited Pt N-layers on the same chip. Data from the junctions on this particular chip will be presented in Figs. 4–10 although results from other chips will be brought into the discussion of results.

Fig. 2(b) shows cross-sections of five test FIB cuts which shows that the in-situ deposited Pt was effective in filling the volume where MgB_2 was removed. The depth of the test cuts shown here were 150% to 400% of the thickness of the MgB_2 film whereas most of our measured devices had cuts that were 100% of the film thickness or less resulting in a gap between MgB_2 electrodes of about 70 nm. A nominal depth of 100% was defined by real-time monitoring of a change in sample current while the FIB cut was being made and was confirmed to roughly correspond to the MgB_2 film thickness by cross-sectional scanning-ion images of the cuts.

III. Results and Discussion

Fig. 4(a) shows I–V curves for a thinned microbridge junction. Josephson characteristics were observed for FIB cuts at 70% and 80% through the film (devices 15–18). The highest temperature for nonzero J_c was 32 K. The parameters for this thinned microbridge junction at 20 K are $I_c = 570$ μA, $J_c = 1.1 \times 10^5$ A/cm^2, $R_n = 0.56\ \Omega$, and $I_cR_n = 319$ μV.

TABLE I
Junction Fabrication Parameters for a Single Chip.

Device number	Depth of cut[a]	In-situ Pt?	Schematic in Fig. 1	Resulting Device Type
1	100%	yes	d	High-value resistor
2	100%	yes	d	High-value resistor
3	90%	yes	c	Weak junction
4	90%	yes	c	Superconducting short
5	80%	yes	c	Jct + excess current
6	80%	yes	c	Jct + excess current
7	70%	yes	c	Jct + excess current
8	70%	yes	c	Jct + excess current
9	60+120%[b]	no	b	High-value resistor
10	60+120%[b]	no	b	Junction
11	100%	no	a	High-value resistor
12	100%	no	a	High-value resistor
13	90%	no	a	High-value resistor
14	90%	no	a	High-value resistor
15	80%	no	a	Junction
16	80%	no	a	Junction
17	70%	no	a	Junction
18	70%	no	a	Junction

[a] 1st FIB cut across entire width of 10 μm bridge
[b] 2nd FIB cut excluded 0.1 μm-wide section of bridge

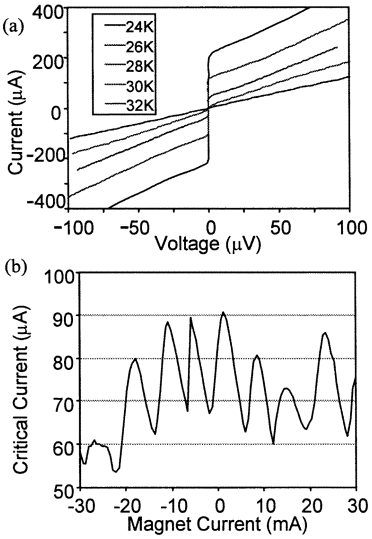

Fig. 4. (a) Current vs. voltage curves at varying temperatures for a thinned microbridge junction. (b) Current vs. magnetic field for same junction where 30 mA of magnet current produced a field of 10 Oe.

For the same junction, Fig. 4(b) shows a substantial but highly nonideal modulation of I_c in magnetic field applied normal to the film, $>$30% modulation in $<$10 Oe. The deviation from Fraunhofer behavior is an indication that current flow through the device is nonuniform. The period of the modulation is about two times smaller than expected from the junction area— including two magnetic penetration lengths [6]—of about 0.4×10 μm. We cannot determine whether that is another sign of nonuniform current flow or an effect of flux-focusing by the MgB_2 junction electrodes.

FIB cuts made 90% or 100% through the film (devices 11–14) resulted in high-value resistors with resistances at 20 K that were two or three orders of magnitude higher than the 70–80% cuts. We speculate that these thinner MgB_2 coupling regions were not superconducting either because the original MgB_2 film had

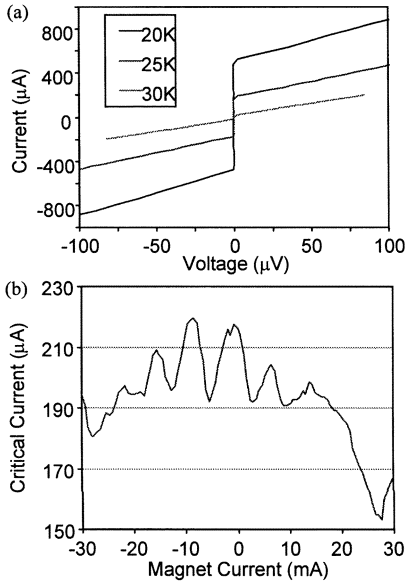

Fig. 5. (a) Current vs. voltage curves at varying temperatures for an SNS junction. (b) Current vs. magnetic field for same junction.

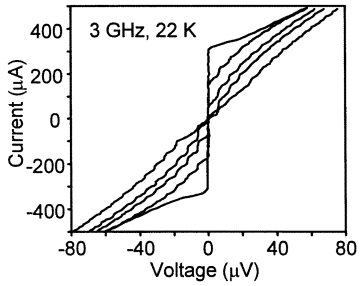

Fig. 6. I–V curves for device 6, SNS junction, in 3 GHz radiation with power levels from -10 dBm to 0 dBm.

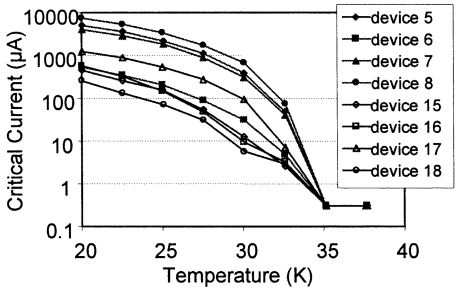

Fig. 7. Critical current vs. temperature for thinned microbridge and SNS junctions. Higher critical currents for the SNS junctions indicate coupling through the Pt N-layer.

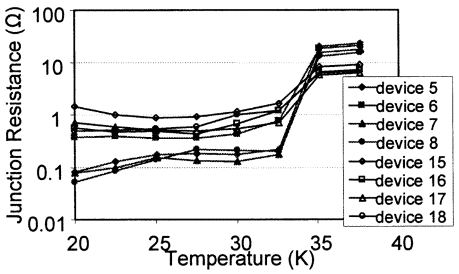

Fig. 8. Junction resistivity vs. temperature for microbridge and SNS junctions.

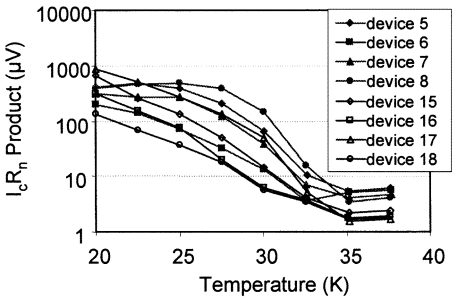

Fig. 9. I_cR_n vs. temperature for microbridge and SNS junctions.

degraded superconducting properties within 20 nm of the substrate interface or exposure to air after FIB processing degraded the thin region.

Fig. 5(a) shows I–V curves for a junction that is nominally SNS-structure. There is some ambiguity about the role of the Pt N-layer since, as we observed for the thinned microbridges, Josephson characteristics were observed for FIB cuts at just 70% and 80% through the film (devices 5–8) and—in just the case of device 3—for a cut 90% through the film. Again, the highest temperature for nonzero J_c was 32 K. The parameters for this nominally SNS junction at 20 K are $I_c = 540$ μA, $J_c = 1.1 \times 10^5$ A/cm^2, $R_n = 0.36$ Ω, and $I_cR_n = 194$ μV. Fig. 5(b) shows $I_c(B)$ for the same junction and indicates highly nonuniform current flow through the junction just as we observed for the thinned microbridges.

Both the shape of the I–V curves and substantial modulation of critical currents in a weak magnetic field indicate Josephson behavior in these devices. In addition, we observed constant-voltage steps in rf fields of 1 to 10 GHz for all of the junctions. An example is shown in Fig. 6 for one of the SNS junctions.

Figs. 7, 8 and 9 show $I_c(T), R_n(T)$, and $I_cR_n(T)$, respectively, for devices 5–8 and 15–18. The first observation for Fig. 7 is that I_c uniformity is poor, even for this small number of junctions, which is consistent with nonuniformity inferred from the $I_c(B)$ measurements. However, Fig. 7 shows consistently higher $I_c(T)$ for the nominal SNS devices indicating that there is some coupling through the Pt N-layer.

The junction resistance is also lower (Fig. 8) for the SNS junctions, consistent with some conduction through the Pt. Note that R_n is roughly independent of temperature for all devices.

The I_cR_n products shown in Fig. 9 for thinned microbridge and SNS junctions are the figure-of-merit that relates to the potential application of these junctions in digital circuits. Although it is encouraging that $I_c > 0$ for temperatures up to 32 K, an I_cR_n product of hundreds of microvolts at 25 K has no advantage over YBCO junctions with similar I_cR_n products at 65–70 K.

Fig. 10 shows I–V curves for the third type of junction that we fabricated, a narrowed microbridge junction. This junction was made by first cutting 60% of the film thickness across the entire 10 μm bridge, and then cutting another 60% of remaining film, leaving behind a 0.1 μm wide by 70 nm long bridge to couple the MgB_2 electrodes. The highest temperature for which a nonzero J_c could be measured was $\sim$14 K, significantly lower than for the other two junction configurations. Two possible reasons for the weak coupling in this type of junction are that the narrowed

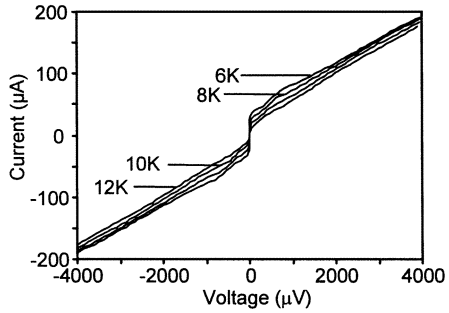

Fig. 10. I–V curves for a 0.1 μm narrowed microbridge junction.

bridge was damaged by the FIB or was degraded by exposure to air.

For all three types of junctions, the fundamental ratio that determines the coupling between MgB_2 electrodes is the distance between electrodes compared to the coherence length in the coupling region. For thinned or narrowed microbridges, the gap created by the FIB, $\geq$70 nm, is about 15 times the superconducting coherence length for MgB_2 [7]. FIB patterning seems unlikely to ever bring this ratio down from 15 to 1–2 so microbridge configurations are ultimately limited in I_cR_n products by this weak coupling.

On the other hand, coherence lengths in clean normal-metals are a good match to the 70 nm scale of FIB cuts. This is the motivation for our SNS junction experiments. The limitation in our work is that the *in-situ* Pt deposition technique that is available in the FIB system contaminates the Pt with Ga, thus increasing its resistivity and reducing its normal-metal coherence length.

The SNS configurations in Fig. 1(c) and (d) are designed to use clean normal-conducting metals to fill the FIB-created gap without exposing the edges of the gap to air. We fabricated devices using the configuration shown in Fig. 1(c) where the first MgB_2/Au interface, one formed on the top surface of the unpatterned MgB_2 film, was prepared in the same vacuum system where we ion-mill cleaned the MgB_2 surface until XPS showed no sign of surface carbon contamination. Nevertheless, the MgB_2/Au contact resistance was much higher than the MgB_2/Pt interface formed in the FIB system. The configuration in Fig. 1(d) addresses that problem but has not been tested experimentally.

IV. Conclusion

We fabricated MgB_2 junctions in three configurations using a focused ion beam (FIB) to create thinned microbridges, narrowed microbridges, and planar SNS structures. We contend that the SNS structure has the best potential for high I_cR_n products since clean Pt or Au have a normal-conductor coherence length that potentially matches the width of the FIB cut while the superconducting coherence length of MgB_2 is too small. However, the Pt deposited in our FIB chamber was not clean enough and resulted in $I_cR_n(20\ \mathrm{K}) \approx 0.5$ mV, the same order as the thinned microbridge junctions. Our process for in-situ ion-cleaning and clean Au deposition failed to achieve contact resistances as low as with the dirty Pt. A proposed solution is to combine in-situ Pt deposition with clean Au deposited outside of the FIB system.

References

[1] J. Nagamatsu, N. Nakagawa, T. Muranaka, Y. Zenitani, and J. Akimitsu, "Superconductivity at 39 K in magnesium diboride," *Nature*, vol. 410, pp. 63–64, 2001.

[2] G. Burnell, D.-J. Kang, H. N. Lee, S. H. Moon, B. Oh, and M. G. Blamire, "Planar superconductor-normal-superconductor Josephson junctions in MgB_2," *Appl. Phys. Lett.*, vol. 79, no. 21, pp. 3464–3466, Nov. 2001.

[3] A. Brinkman, D. Veldhuis, D. Mijatovic, G. Rijnders, D. Blank, H. Hilgenkamp, and H. Rogalla, "Superconducting quantum interference device based on MgB_2 nanobridges," *Appl. Phys. Lett.*, vol. 79, no. 15, pp. 2420–2422, Oct. 2001.

[4] Y. Zhang, D. Kinion, J. Chen, J. Clarke, D. G. Hinks, and G. W. Crabtree, "MgB_2 tunnel junctions and 19 K low-noise dc superconducting quantum interference devices," *Appl. Phys. Lett.*, vol. 79, no. 24, pp. 3995–3997, Dec. 2001.

[5] S. D. Bu, D. M. Kim, J. H. Choi, J. Giencke, S. Patnaik, L. Cooley, E. E. Hellstrom, D. C. Larbalestier, C. B. Eom, J. Lettieri, D. G. Schlom, W. Tian, and X. Q. Pan, Synthesis and properties of c-axis oriented epitaxial MgB_2 thin films, in Appl. Phys. Lett., 2002. to be published.

[6] X. H. Chen, Y. Y. Xue, R. L. Meng, and C. W. Chu, "Penetration depth and anisotropy in MgB_2," *Phys. Rev. B*, vol. 64, pp. 172 501–172 504, July 2001.

[7] D. K. Finnemore, J. E. Ostenson, S. L. Bud'ko, G. Lapertot, and P. C. Canfield, "Thermodynamic and transport properties of superconducting MgB_2," *Phys. Rev. Lett.*, vol. 86, no. 11, pp. 2420–2422, Mar. 2001.